

纳米压痕法测量锌铝钎料的室温蠕变应力指数

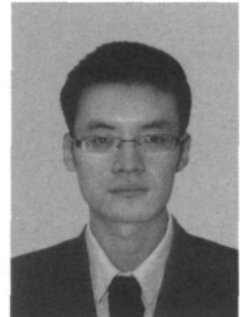
姬 峰¹, 薛松柏¹, 刘 霜¹, 姜继源², 姜银斌²

(1. 南京航空航天大学 材料科学与技术学院, 南京 210016; 2. 浙江新锐焊接材料有限公司, 嵊州 312452)

摘 要: 利用纳米压痕技术, 采用恒加载速率法, 研究了 Zn-22Al 和 Zn-22Al-0.03Ti 钎料的室温蠕变行为, 并对相关数据进行了测量和计算。结果表明, 室温时任一载荷条件下保载时, 钎料均发生了明显的蠕变行为。其中 Zn-22Al-0.03Ti 钎料的压入深度和蠕变位移均小于 Zn-22Al 钎料, 最大差值分别为 15.68% 和 26.87%。相同保载时间不同载荷保载时, 两种钎料的蠕变位移均有较大差异。通过拟合计算分别获得了两种钎料室温时的蠕变应力指数, Zn-22Al-0.03Ti 较 Zn-22Al 提高了 35.79%。分析认为, Ti 元素的添加导致了 Zn-22Al 钎料晶粒的细化, 从而产生了更多的晶界是导致钎料室温抗蠕变能力提高的主要原因。

关键词: 纳米压痕; 锌铝钎料; 蠕变变形; 应力指数

中图分类号: TG425.2 **文献标识码:** A **文章编号:** 0253-360X(2013)02-0075-04



姬 峰

0 序 言

铜铝异种金属接头由于具有优良的导电导热性能、适当的强度、较轻的重量以及较低的成本, 已经在电力电气及制冷等行业得到迅速推广^[1-3]。Zn-Al 系列钎料是众多应用于铜铝异种金属钎焊的材料之一, 其中 Zn-22Al 钎料由于同 AlF₃-CsF 钎剂具有较好的工艺适配性, 已经逐渐开始在电力电气及制冷行业推广使用。微量 Ti 元素的添加已经被证明可以显著细化 Zn-Al 合金的组织, 因此在熔炼 Zn-22Al 钎料过程中通常需要添加微量的 Ti 元素以改善合金的加工性能。

金属材料的蠕变应力指数是评价其蠕变能力的主要指标^[4,5]。不同金属的室温蠕变能力有显著区别, 通常情况下熔点较高的金属室温蠕变能力很低, 用传统的单轴拉伸方法很难准确测量其蠕变应力指数^[6]。纳米压痕仪具有极高的载荷和位移分辨率, 并且不受材料结构和体积的限制, 可以在不破坏材料的前提下, 利用载荷—深度曲线得到硬度、弹性模量等力学参数, 因而被广泛应用于各种材料力学性能测试。纳米压痕仪可以连续记录压头压入材料过程中载荷与深度的变化, 即获得连续的载荷—深度位移曲线。纳米压痕技术具有测试区域精准、微小的

特点, 为材料微观尺寸范围内力学性能的研究提供了很大的便利。

Zn-Al 合金在室温下具有蠕变特性, 属应变速率敏感材料^[7,8], 因此研究其室温蠕变性能对该钎料的应用具有重要意义。试验使用纳米压痕技术, 采用恒加载速率法测量了室温时不同载荷下 Zn-22Al 和 Zn-22Al-0.03Ti 两种钎料的蠕变应力指数, 为进一步研究中温钎料的性能提供相应的数据和理论基础。

1 试验方法及原理

1.1 试验方法

合金用原料纯度(质量分数)为 99.9% 的锌、铝、钛, 熔炼过程在真空炉中进行, 熔炼温度为 750℃ ± 10℃。试样切割精磨后进行机械抛光, 并用超声波清洗去除表面杂质, 以保证试样表面的粗糙度和平整度。

试验采用美国 MTS 公司的 NANOG 200 型纳米压痕仪, 设备压头为金刚石 Berkovich 型压头, 系统压痕和载荷分辨率分别为 0.01 nm 和 50 nN。试验过程包括加载、保载和卸载 3 个阶段, 首先压头先以 10 mN/s 的速度接触试样表面, 再以 2.5 mN/s 的恒定速率加载至最大载荷, 然后在最大载荷下保持 5 min 以获得材料的蠕变特征, 最后再以 10 mN/s 的恒定速率卸载, 待卸载至最大载荷 10% 处时, 保持 1

收稿日期: 2012-07-10

基金项目: 南京航空航天大学大学生创新训练计划资助项目(2012-10287047)

min, 消除热漂移影响. 为获得材料整体力学性能, 试验最大载荷分别选取 50, 80, 100, 200, 300 mN 进行测试. 测试温度为室温, 环境温度波动小于 $\pm 1^\circ\text{C}$. 每组测试条件下对试验重复 3 次测量, 再取平均值. 以上所有测试中相邻压痕之间的距离都超过 500 μm , 避免产生残余应力或引起相邻压痕出现挤压现象.

1.2 试验原理

钎料室温时的蠕变行为可由幂律公式表示, 即蠕变应变率 $\dot{\varepsilon}$ 与施加应力 σ 同测试温度 T 的关系可以简化表示为^[9]

$$\dot{\varepsilon} = A_1 \sigma^n \exp\left(\frac{-Q}{RT}\right) \quad (1)$$

式中: A_1 为材料相关常数; n 为应力指数; R 为气体常数; Q 为蠕变激活能. 纳米压痕条件下, 并不易确定材料的应力及应变关系, 但是在温度及加工硬化能力恒定时, 材料的硬度值 H 和应变速率的关系可以表示为^[10]

$$\dot{\varepsilon}_i = A_2 (H)^n \quad (2)$$

式中: A_2 为材料结构相关比例常数. Berkovich 型压头具有几何相似性, 即在一定载荷范围内, 不同载荷形成的压痕形貌相似, 仅是数值上相差一个特定的尺寸因子. 因此压痕应变速率也可以定义为瞬时压入速率与当前位移的比 \dot{h}/h , 即

$$\dot{\varepsilon} = \dot{h}/h \quad (3)$$

其中,

$$\dot{h} = dh/dt \quad (4)$$

而硬度通常被定义为

$$H = F/A \quad (5)$$

将式(3)~式(5)带入式(2)可得

$$\frac{dh}{dt} \frac{1}{h} = A_2 \left(\frac{F}{A} \right)^n \quad (6)$$

对式(6)两边取对数即可得

$$n = \frac{\partial \ln \dot{\varepsilon}}{\partial \ln H} = \frac{\partial \ln(\dot{h}/h)}{\partial \ln(F/A)} \quad (7)$$

即可求得蠕变因子 n . 值得注意的是, 蠕变后期, 压头应变速率极低, 如果直接采用测量数据 dh/dt 对应力因子进行拟合, 会引入很大误差. 因此需要去除保载后期无效数据点, 采用隔点取点来进行直线拟合, 得到应力因子 n .

2 试验结果及分析

2.1 压痕试验结果

图 1a, b 分别为室温时 Zn-22Al 和 Zn-22Al-0.03Ti 两种钎料在不同最大载荷下的载荷—位移

曲线. 试验结果表明, 在任一载荷情况下, 每个试样都表现出明显的金属材料压痕特性. 即在一定的加载速率下, 随着压入载荷的增加, 压入位移呈非线性增加, 而且有明显的永久变形和不明显的弹性回复. 在最大载荷保持阶段, 蠕变是最主要的变形形式, 即图 1a 中的 BC 段. 但不同组分钎料的压入深度存在明显差别, 两种钎料在不同最大载荷时的压入深度如表 1 所示. 从中可以看出, 两种钎料的压入深度都随最大载荷的增加而逐渐增加, 但是 Zn-22Al-0.03Ti 钎料的最大压入深度始终低于 Zn-22Al. 其中, 当最大加载载荷为 200 mN 时, Zn-22Al-0.03Ti 的压入深度相对 Zn-22Al 降低了 15.68%. 这表明 Zn-22Al 中钛的添加起到了增强钎料基体的作用.

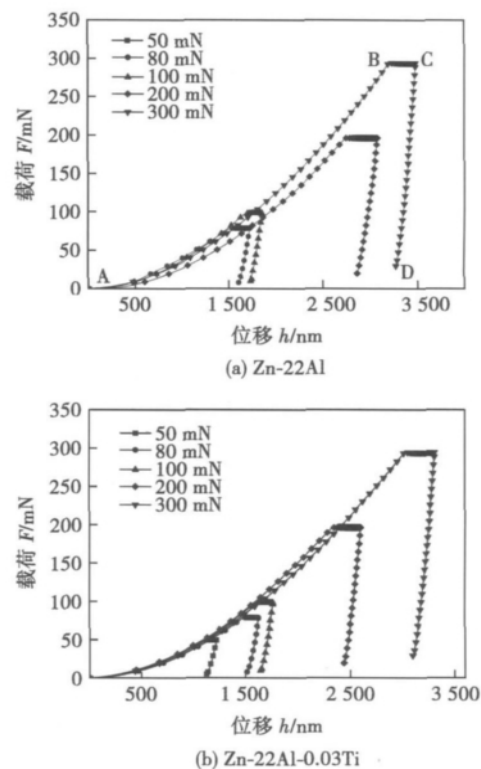


图 1 钎料载荷—位移曲线

Fig. 1 Indentation load vs. depth curves of Zn-22Al and Zn-22Al-0.03Ti filler metals

表 1 不同载荷时钎料最大压入深度 (nm)

Table 1 Depths of filler metals with different loading

载荷 F/mN	Zn-22Al	Zn-22Al-0.03Ti
50	1 439.27	1 221.36
80	1 727.89	1 628.37
100	1 857.31	1 766.78
200	3 082.28	2 598.81
300	3 480.19	3 307.61

2.2 钎料合金蠕变应力指数的确定

最大载荷保持过程中,钎料发生了明显的蠕变行为.图2a、b分别给出了Zn-22Al和Zn-22Al-0.03Ti钎料最大载荷保载期间的蠕变位移—时间曲线.为了方便比较,对最大载荷保载起始阶段的压入深度和时间进行了归零处理.试验结果表明在任一试验条件下,蠕变位移和压入深度都在保载起始阶段有一段快速增长的区间,随后蠕变位移和压入深度虽然继续增加,但是增长速度会逐渐减小,并最终趋于稳定.

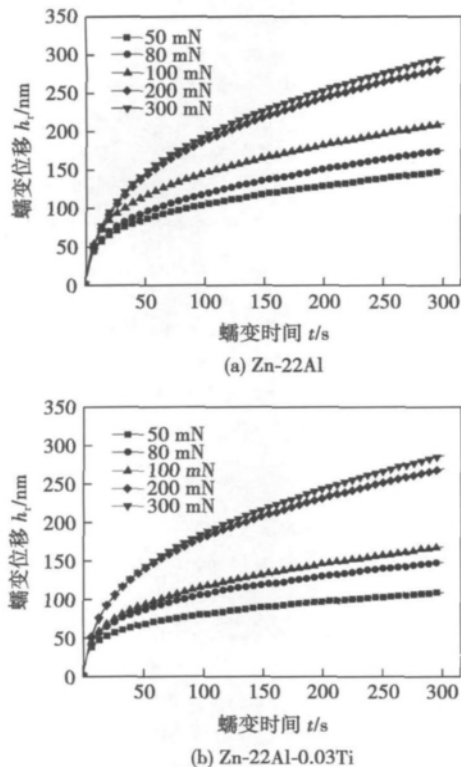


图2 钎料蠕变位移—时间曲线

Fig. 2 Creep displacement vs. time curves of Zn-22Al and Zn-22Al-0.03Ti filler metals

虽然保载时间相同,当最大载荷变化时,钎料的蠕变位移也会有很大不同.从图3可以看出,Zn-22Al和Zn-22Al-0.03Ti两种钎料在最大载荷为300 mN时的蠕变位移分别为50 mN时的1.99倍和2.64倍.这可能是因为在一一定的加载速率下,所施加的载荷越大,钎料在加载变形阶段储存的弹性变形能也越大,而在保载阶段储存的弹性变形能得到释放,相应的塑性变形也就越大.图3还给出了两种钎料在5种最大载荷下的蠕变位移,从中可以看出,在任一载荷下Zn-22Al-0.03Ti的蠕变位移均小于Zn-22Al钎料,当加载载荷为50 mN时,Zn-22Al-0.03Ti钎料的蠕变位移较Zn-22Al减小了26.87%,

表明Ti元素的加入提高了钎料基体的抗蠕变性能.

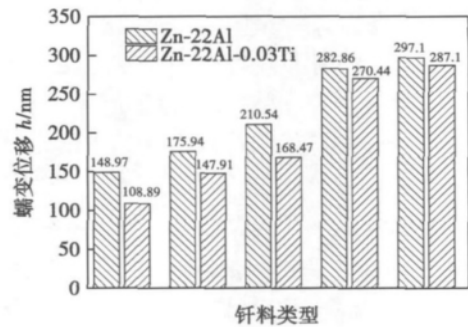


图3 不同最大载荷时的钎料蠕变位移

Fig. 3 Creep displacements of filler metals with different loadings

进一步对二种钎料的室温蠕变应力指数 n 进行求解分析.纳米压痕蠕变试验中,材料的蠕变过程主要与其硬度和加工硬化能力相关,通过单次测量即可获得材料的蠕变应力指数.对两种钎料保载过程中的蠕变位移—时间曲线相关数据按照式(7)进行计算并拟合,其中 $\ln \dot{\epsilon} - \ln H$ 的斜率即为钎料的蠕变应力指数 n ,拟合结果如图4所示.Zn-22Al和Zn-22Al-0.03Ti钎料的蠕变应力指数范围分别位于

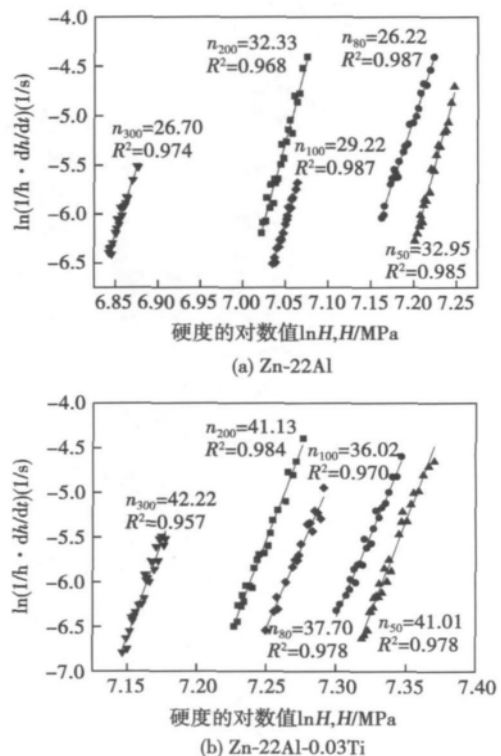


图4 不同载荷时钎料蠕变应力指数

Fig. 4 Double logarithmic plot of creep strain rate vs. hardness of filler metals

26.22 ~ 32.95 和 36.02 ~ 42.22 之间,期间的差异主要是由于环境噪音等条件所引起的试验误差所导致. 拟合结果表明 Zn-22Al-0.03Ti 钎料的蠕变应力指数较 Zn-22Al 提高了大约 35.79%. 当在 Zn-22Al 合金中加入钛后,在此试验的熔炼温度下,熔点较高的钛会以单质形式与凝固过程中优先析出并为富锌相和富铝相提供形核质点,从而细化 Zn-22Al 晶粒. 而有研究表明室温时 Zn-Al 合金中蠕变机制主要为位错攀移^[7,8],细化后的 Zn-22Al-0.03Ti 合金晶粒尺寸要明显小于 Zn-22Al,相对应的晶界数量及长度则大量增加,从而制约了钎料合金的室温蠕变行为,导致了钎料的 n 值增加. 该结果表明 Zn-22Al-0.03Ti 钎料的抗蠕变能力要高于 Zn-22Al,更适宜在震动及压力环境下应用.

3 结 论

(1) 利用纳米压痕技术,采用恒加载速率法,发现 Zn-22Al 和 Zn-22Al-0.03Ti 钎料在载荷保持阶段均发生了明显的蠕变变形,但在任一试验条件下后者的压入深度和蠕变位移均小于前者,其最大差值分别达到 15.68% 和 26.87%.

(2) 使用不同载荷加载时,保载阶段 Zn-22Al 和 Zn-22Al-0.03Ti 钎料的室温蠕变位移均发生较大差异,表现出明显的尺寸效应.

(3) 通过计算获得了 Zn-22Al 和 Zn-22Al-0.03Ti 的室温蠕变指数,其中后者较前者提高了 35.79%,分析认为是晶粒细化引起的晶界数量增加所导致.

参考文献:

- [1] 薛松柏,董 健,吕晓春,等. Al/Cu 管异种材料火焰钎焊连接[J]. 焊接,2003(12): 23-24.
Xue Songbai, Dong Jian, Lü Xiaochun, et al. Flame brazing for dissimilar materials of Al/Cu tube[J]. Welding & Joining, 2003(12): 23-24.
- [2] 张 满,薛松柏,姬 峰,等. CuAl₂ 相对铜铝钎焊接头组织与性能的影响[J]. 焊接学报,2011,32(2): 93-96.

- Zhang Man, Xue Songbai, Ji Feng, et al. Effect of CuAl₂ phase on properties and microstructure of Cu/Al brazed joint[J]. Transactions of the China Welding Institution, 2011, 32(2): 93-96.
- [3] 姬 峰,薛松柏,张 满,等. 时效对铜铝钎焊接头界面化合物和性能的影响[J]. 焊接学报,2012,33(5): 21-24.
Ji Feng, Xue Songbai, Zhang Man, et al. Effects of thermal aging on intermetallic compounds and properties of Cu/Al brazing joint[J]. Transactions of the China Welding Institution, 2012, 33(5): 21-24.
- [4] Liu C Z, Chen J. Nanoindentation of lead-free solders in micro-electronic packaging[J]. Materials Science and Engineering A, 2007, 448(1/2): 340-344.
- [5] Han Y D, Jing H Y, Nai S M L, et al. Temperature dependence of creep and hardness of Sn-Ag-Cu lead-free solder[J]. Journal of Electronic Materials, 2010, 39(2): 223-229.
- [6] 陈 吉,汪 伟,卢 磊,等. 纳米压痕法测量 Cu 的室温蠕变速率敏感指数[J]. 金属学报,2001,37(11): 1179-1183.
Chen Ji, Wang Wei, Lu Lei, et al. Measurement of creep rate sensitivity of copper at room temperature by using nanoindentation[J]. Acta Metallurgica Sinica, 2001, 37(11): 1179-1183.
- [7] 任明星,李邦盛,杨 闯,等. 纳米压痕法测定微铸件室温蠕变速率敏感指数[J]. 金属学报,2008,44(3): 272-276.
Ren Mingxing, Li Bangsheng, Yang Chuang, et al. Measurement of creep rate sensitivity of microcasting at room temperature by using nanoindentation[J]. Acta Metallurgica Sinica, 2008, 44(3): 272-276.
- [8] 李邦盛,任明星,王振龙,等. 微尺度铸件室温蠕变性能的微尺度效应[J]. 机械工程学报,2009,45(2): 178-183.
Li Bangsheng, Ren Mingxing, Wang Zhenlong, et al. Microscale effects on creep properties of microcastings at room temperature[J]. Journal of Mechanical Engineering, 2009, 45(2): 178-183.
- [9] 谭孟曦. 利用纳米压痕加载曲线计算硬度-压入深度关系及弹性模量[J]. 金属学报,2005,41(10): 1020-1024.
Tan Mengxi. Extracting hardness-displacement relations and elastic modulus using nanoindentation loading curves[J]. Acta Metallurgica Sinica, 2005, 41(10): 1020-1024.

作者简介: 姬 峰,男,1987 年出生,博士研究生. 主要从事铝铜和铝钢等异种金属连接的研究. 发表论文 9 篇. Email: jifeng402@163.com

通讯作者: 薛松柏,男,博士,教授,博士研究生导师. Email: xuesb@nuaa.edu.cn

strengthen the interface by controlling the holding time.

Key words: Ti_3Al -based alloy; transient liquid phase diffusion bonding; interface

Measurement of creep stress exponent of Zn-Al filler metal at room temperature by using nanoindentation JI Feng¹, XUE Songbai¹, LIU Shuang¹, LOU Jiyan², LOU Yinbin² (1. College of Materials Science and Technology, Nanjing University of Aeronautics and Astronautics, Nanjing 210016, China; 2. Zhejiang Xinrui Welding Material Co., Ltd, Shaoxing 312400, China). pp 75 – 78

Abstract: The creep behavior of Zn-22Al and Zn-22Al-0.03Ti filler metals at room temperature were studied by nanoindentation in this paper, and constant loading rate method was used to calculate the creep stress exponent. The results indicate that, both the Zn-22Al and Zn-22Al-0.03Ti produced obvious creep deformation under holding load. Both the depth and creep displacement of Zn-22Al-0.03Ti were less than that of Zn-22Al, and the maximum difference were 15.68% and 26.87%, respectively. Under the constant time, the filler metals produced different creep displacement with different loadings. The creep stress exponents of two filler metals at room temperature were obtained by fitting method. Zn-22Al-0.03Ti had a higher creep stress exponent than Zn-22Al filler metal, which implied that Ti-bearing filler metals had better creep resistance than Zn-22Al alloy. The grain of Zn-22Al filler metal could be refined remarkably with the Ti addition, which might result in the increase of grain boundary and finally enhanced the creep resistance of alloy.

Key words: nanoindentation; Zn-Al filler metal; creep; creep stress exponent

Structure and mechanical properties on DH40 ship building steel joints by multi-layer and multi-pass welding technology

LU Xuedong¹, CEN Yue², WANG Huan², WU Mingfang¹ (1. Provincial Key Lab of Advanced Welding Technology, Jiangsu University of Science and Technology, Zhenjiang 212003, China; 2. HuDong-ZhongHua Ship Building Company Limited, Shanghai 200129, China). pp 79 – 83

Abstract: The weldability experiments of DH40 ship building steel were carried out by using the flux-cored wire CO_2 gas shielded multi-pass welding technology. The microstructure and mechanical properties of the joint were studied systematically and the impact toughness was discussed, especially the reason why the impact toughness at HAZ of 5 mm from fusion line of weld root decreased greatly. The results showed that the tensile strength of joints is higher than that of the base metal of 575 MPa. All the samples used in the bending test are qualified and meet the plasticity requirement. The brittleness band is easily formed at HAZ, 5 mm from the fusion line at the weld root. The effect of microstructure heredity results in the coarse crystal grain, which is the secondary reason for the impact ductility decreasing, and the basic reason is the formation of a large amount of granular bainite.

Key words: DH40 steel; multi-pass welding technology; mechanical properties; microstructure

Effect of process parameters on mechanical properties of friction stir welded Al-Li alloy lap joints ZHANG Dan-

dan¹, QU Wenqing¹, YIN Na¹, YANG Mucong², CHEN Jie², MENG Qiang³, CHAI Peng³ (1. School of Mechanical Engineering and Automation, Beihang University, Beijing 100191, China; 2. Shanghai Aircraft Manufacturing Co., Ltd, Shanghai 200436, China; 3. National FSW Center, Aeronautical Manufacturing Technology Research Institute, Beijing 100024, China). pp 84 – 88

Abstract: Through analyzing the microstructure and testing mechanical properties of friction stir welded Al-Li alloy lap joints, the effect of FSW welding parameters on the tensile properties of the lap joints was investigated. The results showed that the length of stir pin has significant influence on the tensile properties of lap joints. When the length of pin is changed from 2.8 mm to 2.5 mm, the ultimate strength and elongation of lap joints are obviously improved. Furthermore, the rotation speed / welding speed (η) also affected the performance of joints. When there was a small increasing in η , the tensile properties of lap joints increased accordingly. For the Al-Li alloy lap structure, the optimum tool rotational speed is 800 r/min, welding speed is 200 mm/min and the length of pin is 2.5 mm, the ultimate strength of lap joint reaches 467 MPa, which is equivalent to 94% that of the base metal and the elongation is 3.18%. In addition, the analysis of tensile fracture appearance indicated that the tensile cracks initiate from the location of "Hooking" defect in the advancing side and grow along the HAZ until to the base metal.

Key words: friction stir welding; aluminum-lithium alloy (Al-Li); tensile properties; fracture

Test and analysis of dynamic process for spot welding of multilayer low carbon steel sheets LI Guizhong, DING

Jian, QIN Yuchan, WANG Wenquan (School of Materials Science and Engineering, Jilin University, Changchun 130025, China). pp 89 – 92

Abstract: In the spot welding process, the spot-welded joints of multilayer sheets were always available. The variation of the sheet thickness is obvious in the spot welding process, which makes the impedance fluctuation drastic in secondary circuit of welding power transformer. Thus, the spot welding heat also fluctuates evidently. In this case, the nugget quality cannot be guaranteed if welding heat is not regulated effectively in real time. By means of dynamic test and analysis of welding thermal process, the applicability of different monitoring methods was discussed for spot welding of multilayer low carbon steel sheets. The scientific basis therefore can be provided for manufacturing enterprises to select the exact monitoring method and to achieve the effective quality control.

Key words: low carbon steel; multilayer sheets; spot welding; dynamic process; monitoring method selection

Numerical simulation of metal plastic flow in friction stir welding affected by pin shape JI Shude¹, MENG Qing-

guo³, SHI Qingyu², ZHANG Liguol¹, ZOU Aili¹ (1. Faculty of Aerospace Engineering, Shenyang Aerospace University, Sheny-